ORIGINAL PAPER

Enantioselective recognition of esomeprazole with a molecularly imprinted sol–gel-based electrochemical sensor

Leyla Karadurmus[1,2] · M. Emin Corman[1,3] · Lokman Uzun[4] · Sibel A. Ozkan[1]

Abstract

A simple, selective, and accurate electrochemical chiral sensor based on molecularly imprinted polymer (MIP) has been developed for sensitive and selective detection of esomeprazole (ESOM). For this purpose, the porous MIP sensor was prepared using tetraethyl orthosilicate (TEOS) and cetyltrimethylammonium bromide (CTAB) in the presence of β-cyclodextrin (β-CD) as a chiral recognizing element on a glassy carbon electrode (GCE). The changes in the MIP-layer related to removal and rebinding of the target ESOM were performed via differential pulse voltammetry (DPV) and cyclic voltammetry (CV) by using $[Fe(CN)_6]^{3-/4-}$ as the redox probe. The structures of the developed sensor surface were characterized by using scanning electron microscopy (SEM) and Fourier transform infrared spectroscopy (FTIR). Electrochemical impedance spectroscopy (EIS) was also utilized for a complementary electrochemical characterization. The calibration curve was obtained in the range 1.0×10^{-14}–2.0×10^{-13} M with a limit of detection (LOD) of 1.9×10^{-15} M. The developed method has improved the accessibility of binding sites by producing the porous material via hydrolysis/condensation reaction of TEOS in presence of CTAB. The selectivity tests of the developed SiO$_2$-β-CD@MIP/GCE sensor indicated a high specificity towards ESOM compared with structurally related competitor molecules such as R-omeprazole (R-OM), R-lansoprazole, and S-lansoprazole. The developed sensor was successfully used to determine ESOM in tablets and commercial human serum samples with satisfactory recoveries (100.25 to 100.60%) and precision (RSD 0.46 to 0.66%).

Keywords Molecularly imprinted polymers · Esomeprazole · Glassy carbon electrode · Electrochemical impedance spectroscopy · Differential pulse voltammetry · β-cyclodextrin · Chiral sensor

Introduction

More than half of the drugs in use in today's pharmaceutical market contain chiral compounds. Still, most of these drugs are administered as a racemic mixture, a 50/50 mixture of their enantiomers [1]. Omeprazole (OME), which irreversibly blocks H$^+$-K$^+$ ATPase enzymes (proton pumps), is the first proton pump inhibitor (PPI) (Scheme 1). Esomeprazole (ESOM) has individual metabolic features that clearly distinguish it from the racemate omeprazole. These features have led to various clinical advantages, such as higher bioavailability at comparable doses in most patients [2, 3].

Nowadays, the significance of developing analytical methods and sensors for enantiomers is well recognized in the chemical and pharmaceutical industries. Several techniques, including electrochemical and optical sensors, high-performance liquid chromatography, capillary electrochromatography, capillary electrophoresis, and supercritical fluid chromatography, have been used for this purpose. Chiral sensors are devices that can recognize and determine the amounts of enantiomers within a sample or racemic mixture. A chiral sensor usually consists of the enantioselective recognition surface and a transducer element. Various modifications may be applied to enhance the specificity of the recognition part [4]. Among these modifications, MIPs are considered the most promising material because of their many advantages, including easy preparation, and relatively

✉ Sibel A. Ozkan
   ozkan@pharmacy.ankara.edu.tr

1   Department of Analytical Chemistry, Faculty of Pharmacy, Ankara University, Ankara, Turkey

2   Department of Analytical Chemistry, Faculty of Pharmacy, Adıyaman University, Adıyaman, Turkey

3   Department of Biochemistry, Gulhane Faculty of Pharmacy, University of Health Sciences, Ankara, Turkey

4   Department of Chemistry, Faculty of Science, Hacettepe University, Ankara, Turkey

Scheme 1 The chemical structure of **a** esomeprazole (ESOM) and **b** r-omeprazole (R-OM)
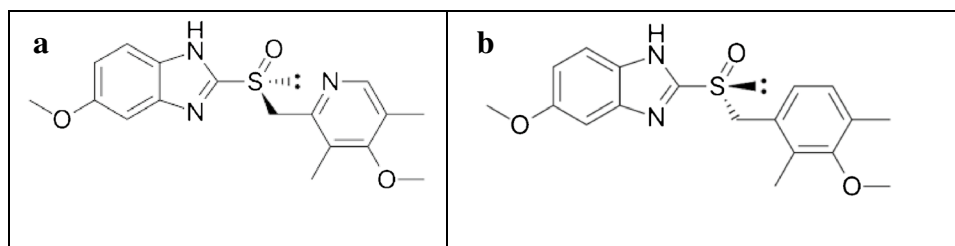
low cost [5–7]. In general, MIP-based chiral sensors are produced by combining MIP polymers onto the surface of the transducer, and changes to the polymer matrix, such as interaction or binding with the target analyte, can be converted into a measurable signal [8]. Various measurement techniques can be used in signal transmission, such as electrochemical or optical ones. Adsorption capacity, stability, and mechanical stability as restriction factors need further optimization using nanomaterials in near future studies.

Up to now, several methods have been established for the detection of ESOM in pharmaceutical dosage forms and biological samples. These developed methods include high-performance liquid chromatography (HPLC) [9–12], gas chromatography [13], electrochemical [14–18], and spectrophotometry [19, 20]. One of them of these electrochemical sensors was developed for simultaneous analysis of ESOM and diclofenac sodium [11]. This developed sensor is a carbon paste electrode (CPE) modified with reduced graphene oxide and Co(OH)2 nano-flakes [12]. Electrochemical sensor has been developed for ESOM based on the synergistic effect of zirconia and polyaniline nanomaterials [13]. The electrochemical analysis of esomeprazole was achieved through the application of SWV on gold electrode [14]. The ESOM was investigated at screen printed carbon electrode using CV and DPV. β-CD and L-arginine modified screen printed carbon electrode was proposed for the detection of ESOM [15]. Each method has its well-known performance in terms of high selectivity and sensitivity. However, some drawbacks like being time-consuming, laborious, or expensive are inevitable for traditional methods.

Herein, we chose CD as a recognition element/functional monomer because of its structural features. As comprehensively reported in literature, CDs and their derivatives have been successfully used in the fabrication of MIP to create high-affinity recognition sites hence improving the selectivity of the resulting MIP. First, the multiple interactions between CD and guest molecules could provide various recognition sites in the CD-based MIPs and hence improve the imprinting ability of the MIPs toward target template molecules, especially for small target molecules. Second, MIPs based on native CD have good adaptability in water medium because of the multiple hydroxyl groups on CDs, which greatly broadens their applications in the food and medicinal industries. The hydroxyl groups of CDs can also be substituted by the

various functional group to modulate the solubility, polarity, recognition ability, and other desired properties of the resulting MIPs. Finally, CD could interact with guest molecules in the form of monomers, dimers, and even multimers in some special cases, which endows MIP diverse recognition patterns to adapt to different template molecules [21].

In this study, cyclodextrin (CD) was used as a functional monomer for the preparation of molecularly imprinted polymer (MIP) in this research. Herein, β-CD was used as a functional monomer to form an inclusion complex with esomeprazole by means of host–guest complexation, while TEOS allows to form porous 3D networks and CTAB as a surfactant lead to the formation of the porous silica particles with tailored pore sizes.

In the present work, a simple, highly sensitive, and selective MIP-based electrochemical chiral sensor was proposed for the detection of ESOM. The sensor was prepared using β-cyclodextrin (β-CD), tetraethyl orthosilicate (TEOS), and cetyltrimethylammonium bromide (CTAB) in the presence of template ESOM molecules via initiating the reaction via the addition of ammonium hydroxide on the GCE. DPV and CV were performed to follow the changes in the MIP layer related to removal and rebinding of the target ESOM by using $[Fe(CN)_6]^{3-/4-}$ as the redox probe. The selectivity tests of the proposed MIP indicated a high specificity towards ESOM compared to other similar molecules. Additionally, the proposed sensor was successfully used to detect ESOM in tablets and biological samples with a good recovery. It should be noted that this study is, to our knowledge, the first report of chiral ESOM detection by the molecularly imprinted polymer.

Experimental

Chemicals and reagents

β-cyclodextrin (β-CD), esomeprazole (ESOM), R-omeprazole (R-OM), S-lansoprazole, R-lansoprazole, drug-free human serum, acetic acid (HAc), acetonitrile (ACN), hydrochloric acid (HCl), tetraethyl orthosilicate (TEOS), and cetyltrimethylammonium bromide (CTAB) were purchased from Sigma-Aldrich (St. Louis, MO, USA). Tripotassium hexacyanoferrate $[K_3Fe(CN)_6]$ and tetra potassium hexacyanoferrate $[K_4Fe(CN)_6]$ were supplied from Merck and used

to prepare the mixture of 5 mM [Fe(CN)$_6$]$^{3-/4-}$ (1:1) in 0.1 M KCl solution as redox probe. All samples used in the experiments were prepared with double-distilled water (Millipore Milli-Q system). The phosphate buffer (PB, pH 7.4) has been used as a supporting electrolyte and stabilizer of the pH of ESOM standard solutions in electrochemical analysis. The 10-mM stock solution of ESOM was diluted to different concentrations with PB (pH 7.4). All these solutions were kept under refrigerated conditions at 4 °C until use.

Equipment

The electrochemical instrument was used AUTOLAB-PGSTAT100 (Eco Chemie, Utrecht, The Netherlands) running with NOVA 2.1.4 software. The electrochemical cell consisted of a conventional three-electrode system with platinum wire as the auxiliary electrode, saturated Ag/AgCl (ASi Research Product, USA) as reference electrode, and GCE (d = 3 mm, BASi Research Product, USA) as the working electrode. CV and DPV were performed in 0.1 M KCl containing 5.0 mM [Fe(CN)$_6$]$^{3-/4-}$ (1:1) from −0.3 to 0.6 V. The pH of solutions were checked by a pH meter (Mettler-Toledo, Switzerland). The removal and rebinding process was realized with Thermo-Shaker (Biosan TS-100, Riga, Latvia). To obtain the precision balance, the chemicals were weighed by Ohaus Instruments (Shanghai, China).

The FTIR spectra were obtained using a Perkin Elmer Spectrum Two™ spectrophotometer using the ATR method in the frequency region of 400–4000 cm^{-1}. The morphological structure of the sensor surface was examined using scanning electron microscopy (SEM) (TESCAN GAIA 3, Brno–Kohoutovice, Czech Republic).

Preparation of the porous polymeric film

Before polymerization, the bare GC electrode was sonicated in an ultrasonic bath in ethanol:water (1:1 v/v) mixture. Next, the bare GCEs were polished in a 1.0-µm alumina suspension and subsequently cleaned with double-distilled water. The molecularly imprinted porous polymeric film was produced as follows: A homogeneous solution including pre-polymerization complex of ESOM:β-CD (1:1 by mole, 0.04 mL, 10^{-3} M), CTAB (0.02 mL, 0.045 mM), and NH$_4$OH (0.02 mL) were mixed for 15 min under the room temperature. After, TEOS:EtOH (1:1 v/v, 100 µL) was added and mixed for 1 min. A drop of this solution (3.0 µL) was added onto the surface of the GCE. Polymerization was performed at the oven (50 °C) for 30 min. After polymerization, the electrode was rinsed with distilled water to expose the pores from the obtained polymeric structure.

Afterward, ESOM was removed from the polymeric structure by acetic acid (HAc, 10 M) treatment at 350 rpm (Thermo-Shaker) at 25 °C for 15 min. Lastly, a determined amount of ESOM was rebound to the developed sensor using the thermo-shaker at 350 rpm at 25 °C for 15 min. Before each incubation, the electrode was rinsed with distilled water for 60 s. The modified electrode, SiO$_2$-β-CD@MIP/GCE, can be reutilized by washing it with distilled water for 60 s before each experiment and used as a cleaned electrode.

Meanwhile, a non-imprinted sensor (NIP/GCE) was synthesized by following the same synthesis route except the absence of ESOM to assess imprinting performance. The convenience of the developed SiO$_2$-β-CD@MIP/GCE chiral sensor was controlled by using the NIP/GCE. Like SiO$_2$-β-CD@MIP/GCE, all electrochemical experiments with NIP/GCE were carried out in [Fe(CN)$_6$]$^{3-/4-}$ mixture.

Preparation of serum and tablet samples

To evaluate the sensor performance in natural samples, the proposed SiO$_2$-β-CD@MIP/GCE sensor was used to detect ESOM in commercial serum samples. Commercial serum samples were stored frozen until the analysis. After thawing a 3.6-mL aliquot of commercial serum sample, it was spiked with 1.0 mL of 0.1 mM ESOM. A 5.4-mL of acetonitrile (ACN) was added to a total volume of 10 mL. The blank serum was prepared with 1.0 mL of 0.1 mM PB (pH 7.4), 3.6 mL of commercial serum sample, and 5.4 mL of ACN. The final mixtures were centrifuged for 20 min at 3500 rpm for removal of protein residues, and then, the supernatants were gathered. In the electrochemical detection, aliquots from the stock mixture of serum were utilized for rebinding of ESOM. The 0.1-mM ESOM concentration was added to the commercial serum sample. Appropriate volumes of this supernatant were transferred into the volumetric flask and diluted up to the volume with phosphate buffer at pH 7.4. The concentration of ESOM was varied in the range of 1×10^{-14}–1×10^{-13} M in human serum samples. Quantifications were performed by means of the calibration curve method from the related calibration equation. The five successive experiments were done with the same sensor and solution. Relative standard deviation (RSD) was assessed to be suggesting good repeatability, and reproducibility of the proposed sensor.

For determination in the tablets, the mean weight of ten tablets, each including 60 mg of ESOM, was measured; then, they were pulverized in a mortar. 1.0 mM stock solution was prepared in water with sonicating at 30 min and subsequently filtered. A certain portion was taken from this filtered solution, and it was diluted in PB (pH 7.4). To examine the amount of ESOM in tablets, recovery investigations were carried with by adding a known amount of pure ESOM to known tablet concentrations and examined by DPV measurements. To study the accuracy of the proposed method and check the possible interferences from common excipients, recovery studies were carried out. For these experiments,

known amount of the pure drug was added to the earlier analyzed tablet formulation of ESOM. The recovery of the drug was calculated using the corresponding regression equations of previously plotted calibration plots.

Selectivity

The developed SiO$_2$-β-CD@MIP/GCE sensor was prepared using 1 mM ESOM as a template and the same rebinding process was utilized. The rebinding step was carried out in solutions containing R-OM, R-Lansoprazole, and S-Lansoprazole as selected similar compounds.

Results and discussion

Characterizations of SiO$_2$-β-CD@MIP/GCE

ATR-FTIR investigation of the sensor surface was performed to confirm the functionalization of SiO$_2$ with β-CD.
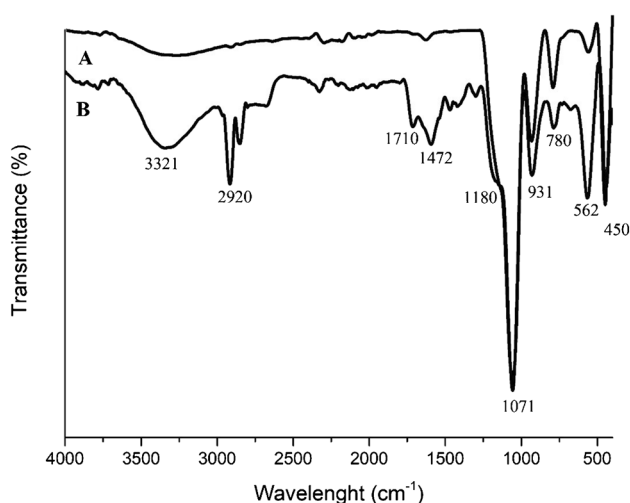
Fig. 1 FTIR-ATR spectra of SiO$_2$ (A) and SiO$_2$-β-CD@MIP/GCE (B) sensor surface
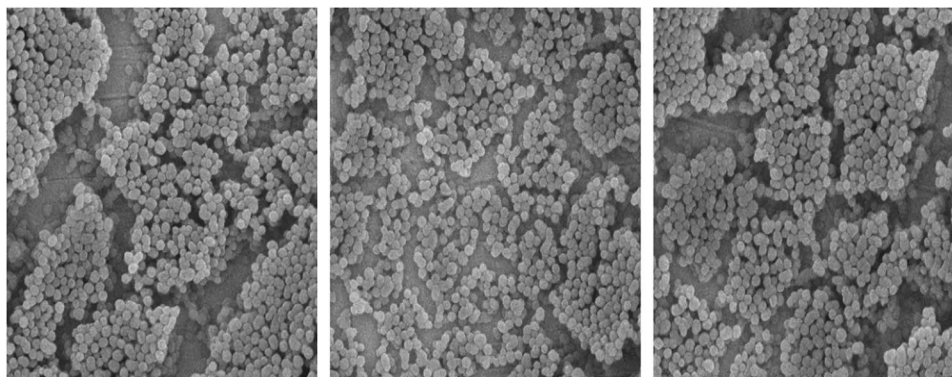
Figure 1A shows the main characteristic band of silica materials at 455 cm^{-1}, 780 cm^{-1}, 931 cm^{-1}, and 1071 cm^{-1} that reveal a dominant band attributed to Si–O–Si bending, Si–O symmetric stretching, Si–OH stretching, and Si–O–Si asymmetric stretching, respectively [22]. Moreover, the common SiO$_2$ bands almost matched up for β-CD modified sensor surface (SiO$_2$-β-CD@MIP/GCE) in Fig. 1B. On the other hand, the typical bands for β-CD incorporated SiO$_2$-β-CD@MIP/GCE are different from those that were detected for SiO$_2$. The SiO$_2$-β-CD@MIP/GCE displayed specific bands at 3321 cm^{-1} (-OH stretching), 2920 cm^{-1} (C-H stretching), 1710 cm^{-1} (carbonyl stretching vibration of ester groups), 1472 cm^{-1} (C-H bending), 1180 cm^{-1} (C-O stretching), and 562 cm^{-1} (skeletal vibration of β-CD) which exhibited the presence of the β-CD [23]. These results confirmed the β-CD was successfully formed on the sensor surface and incorporated into the SiO$_2$ network. SEM measurements were carried out to observe the morphological structure of the synthesized sensor surface. In Fig. 2, the image of SiO$_2$-β-CD@MIP/GCE illustrates the sphere-like morphology of the recognition element. Figure 2 demonstrates the synthesized SiO$_2$ particles with ordered spherical morphology, and porous structure was well attached to the sensor surface.

Electrochemical characterization

For electrochemical characterization of the SiO$_2$-β-CD@MIP/GCE electrodes, EIS and CV methods were applied compared to the results of bare GCE after electropolymerization, removal, and rebinding of ESOM. CV characterization was performed from -0.3 to 0.6 V with a scan rate of 50 mV/s in 0.1 M KCl solution containing 5.0 mM [Fe(CN)$_6$]$^{3-/4-}$. As presented in Fig. 3, bare GCE has the maximum peak current of the [Fe(CN)$_6$]$^{3-/4-}$, whereas the response of [Fe(CN)$_6$]$^{3-/4-}$ cannot be acquired because of the inhibited electron transfer by polymer development after hydrolysis/condensation of TEOS coverage. After removing ESOM from the porous structure, the [Fe(CN)$_6$]$^{3-/4-}$ response was acquired once again, showing

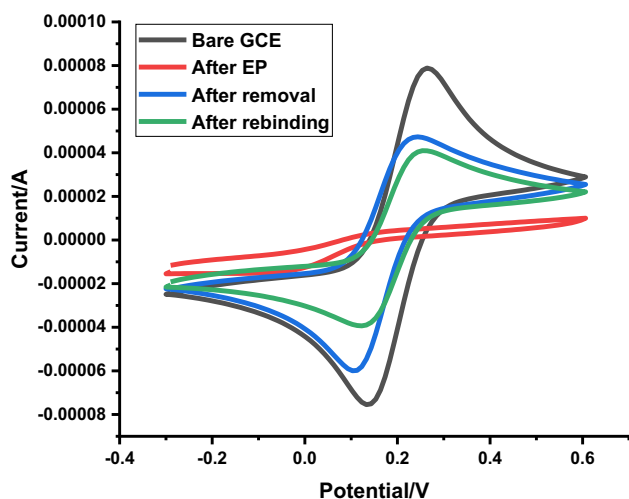**Fig. 2** The SEM images of various electrodes of SiO$_2$-β-CD@MIP/GCE sensor

Fig. 3 CV of each step of the proposed SiO_2-β-CD@MIP/GCE sensor in 5.0 mM $[Fe(CN)_6]^{3-/4-}$ with 50 mV/s

the formation of cavities permitting rebinding and increased electron transfer. Finally, after rebinding of ESOM, a considerable reduction on the $[Fe(CN)_6]^{3-/4-}$, the response was observed because of the reduction/occupation of appropriate binding cavities for $[Fe(CN)_6]^{3-/4-}$ couples.

EIS is another significant technique for the characterization of sensor procedure and effective comparison of the modified and unmodified electrode surface features. EIS was performed at 0.1 M KCl solution containing 5.0 mM $[Fe(CN)_6]^{3-/4-}$ as well (Fig. 4). It can be monitored in fast electron transfer kinetics for the bare GCE. After silicate coverage of the surface, the characteristics of the un-eluting MIP film insulation show blocking effect, and the surface
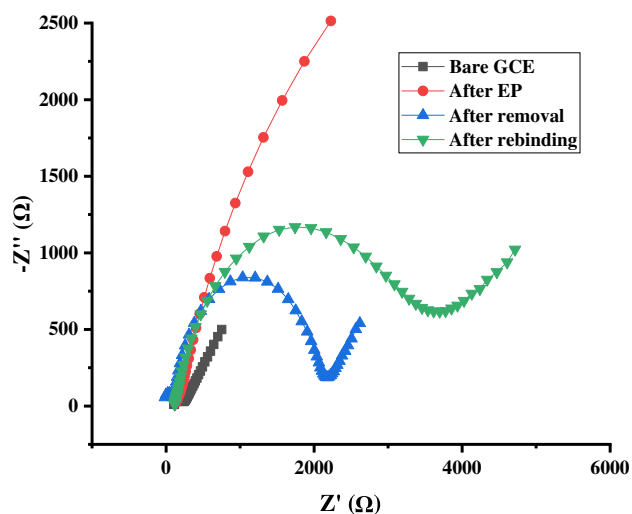
is extremely insistent to electron transfer. The semicircle diameter of the Nyquist diagram increased after dense surface coverage. Furthermore, the removal of ESOM, in other words the resistant, creates imprinted holes in the MIP coverage, and its electron transfer impedance will be lower relative to the MIP. Meanwhile, the rebinding of ESOM allowed recombination into the imprinted holes and occupation of the porous region in the silicate network with a large number of template molecules, which resulted in the high impedance due to the non-conductivity of the template molecules. This outcome can be interpreted as the porous matrix having sufficient capacity to reattach ESOM molecules. Finally, these results coincide with CV results.

Imprinting factor

The selectivity of the SiO_2-β-CD@MIP/GCE sensor was studied by measuring its response towards similar compounds such as R-OM, R-lansoprazole, and S-lansoprazole. SiO_2-CD@MIP/GCE signal was compared with DPV results using 5×10^{-14} M of similar compounds such as R-OM, R-lansoprazole, and S-lansoprazole (Fig. 5).

The selectivity of SiO_2-β-CD@MIP/GCE was assessed using the imprinting factor (IF). IF is determined as the ratio of $\Delta I(I-I_o)$ response of DPV related to MIP and NIP sensor. Imprinting factors (IFs) were calculated using the following equation:

$$IF = \Delta I(MIP)/\Delta I(NIP)$$

Herein, $\Delta I = I_o - I$, where I_o and I are the peak signals of the designed electrode after removal and rebinding of ESOM, respectively. As can be seen from Fig. 5, the IFs of the SiO_2-β-CD@MIP/GCE sensor was 5.81, 1.33, 1.03, and 1.26 for ESOM, R-OM, S-lansoprazole, and R-lansoprazole, respectively. These results demonstrated that the
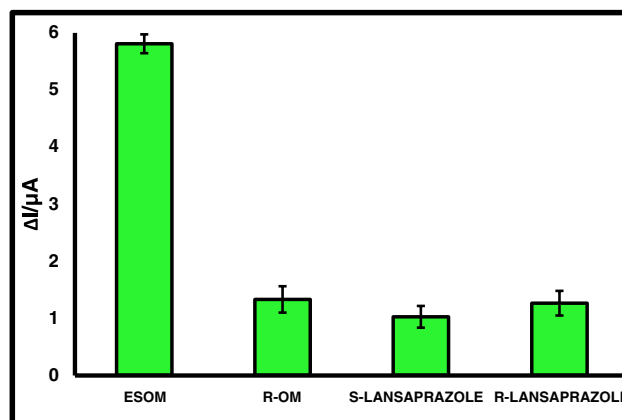

Fig. 4 The EIS corresponding in each step of the formation of SiO_2-β-CD@MIP/GCE sensor

Fig. 5 The evaluation of IF values for ESOM and the similar compounds such as R-OM, S-lansoprazole, and R-lansoprazole

SiO_2-β-CD@MIP/GCE sensor has a specific recognition capability for ESOM compounds.

Analytical performance of SiO_2-β-CD@MIP/GCE sensor

The analytical curve of ESOM was used to evaluate the analytical performance of SiO_2-β-CD@MIP/GCE. The peak signal of SiO_2-β-CD@MIP/GCE was obtained using the anodic peak current at 0.16 V with DPV on the redox probe $[Fe(CN)_6]^{3-/4-}$ after incubation of different concentrations of ESOM.

A linear relationship between ΔI and ESOM concentrations was found between 1×10^{-14} and 2×10^{-13} M, which exhibits the following linear regression equation: ΔI $(A) = 1.73 \times 10^{14} C (M) + 34.572$ ($r = 0.995$) (Fig. 6).

LOD and LOQ were calculated using the slope value of the calibration equation and the standard deviation obtained from at least 5 measurement results of the response of the analyte at the lowest concentration in the calibration curve [18, 19]. LOD and LOQ were found to be at 1.89×10^{-15} M and 6.32×10^{-15} M, respectively.

The DPV of after rebinding of different concentrations of ESOM on the SiO_2-β-CD@MIP/GCE is shown in Fig. 6. The DPV peak current was reduced due to the occupation of specific cavities with ESOM compounds when a higher amount of ESOM was rebound.

The NIP was used for the comparison of the developed SiO_2-β-CD@MIP/GCE sensor. As seen in Fig. 6, the ΔI results stay nearly unaffected when the various amounts of ESOM were rebound, which the non-retention of the ESOM can comment.

Application of the SiO_2-β-CD@MIP/GCE in commercial serum samples and tablet dosage forms

The applicability of the developed sensor was assessed by applying it to commercial serum samples and tablet dosage forms. The application performance of the developed sensor was estimated using the spiking and recovery method. As summarized in Table 1, the obtained recovery percentages confirm the high ability of this method to measure ESOM even in the complex real samples. The good linearity between Ip and C was noticed with LODs (Tables 1 and 3) and quantitative ESOM recoveries (Table 2). Figure 7 shows that the practical utility of the SiO_2-β-CD@MIP/GCE and NIP/GCE sensors was confirmed by defining the concentration of ESOM using the standard addition technique in human serum samples. The SiO_2-β-CD@MIP/GCE and NIP/GCE were immersed in synthetic serum samples with varied ESOM concentrations from 1×10^{-14}–1×10^{-13} M with the linear regression equation of $\Delta I (\mu A) = 2.02 \times 10^{14}$
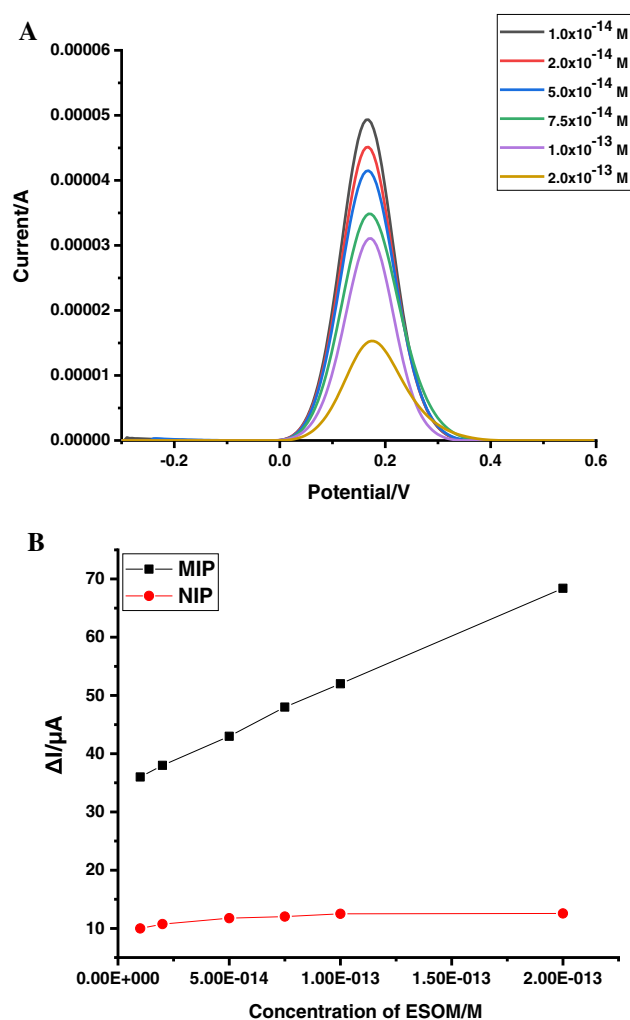
Fig. 6 DPV of ESOM on the SiO_2-β-CD@MIP/GCE (**A**) and a linear relationship between the ΔI and ESOM concentrations in SiO_2-β-CD@MIP/GCE and NIP/GCE (**B**) in 5.0 mM $[Fe(CN)_6]^{3-/4-}$

$C(M) + 45.613$ ($r = 0.993$) using 5 mM $[Fe(CN)_6]^{3-/4-}$ solution as the redox probe. The LOD and LOQ values were calculated as 1.29 fM and 4.27 fM, respectively. The regression data, calibration graph, and DPV curves related to rebinding of different concentrations of ESOM are given in Table 1 and Fig. 7, respectively [24, 25]. Good recovery results were also obtained with the proposed sensor (Table 2).

As shown in Table 2, the recoveries were detected as 100.25% and 100.60%, and relative standard deviation (RSD) was as 0.46% and 0.66% in pharmaceutical dosage forms and synthetic serum samples, respectively. Recent electrochemical studies about esomeprazole are tabulated in Table 3.

Interference studies

The anti-interference ability of proposed SiO_2-β-CD@MIP/GCE sensor was evaluated by detecting ESOM alone and

Table 1 Validation parameters of SiO$_2$-β-CD@MIP/GCE sensor in standard solution and commercial serum sample

Parameter	Standard solution	Serum sample
Linearity range (M)	1×10^{-14}–2×10^{-13}	1×10^{-14}–1×10^{-13}
Slope (μA M^{-1})	1.73×10^{14}	2.02×10^{14}
Standard error of slope	0.27	0.30
Intercept (μA)	34.572	45.613
SE of intercept	2.6	5.2
Correlation coefficient (*r*)	0.99	0.99
LOD (M)	1.89×10^{-15}	1.29×10^{-15}
LOQ (M)	6.32×10^{-15}	4.27×10^{-15}
Repeatability of peak current (RSD%)[a]	0.32	0.54
Reproducibility of peak current (RSD%)[a]	0.52	0.75

[a]Each value is the mean of three experiments

**Table 2** Analysis results of ESOM detection in tablet dosage form and spiked human serum samples

	Tablet dosage form	Serum sample
Label amount (mg)	40.00	–
Found amount (mg)	40.20	–
RSD%[a]	0.76	–
Bias%	0.50	–
Spiked amount (mg)	20.00	5.00
Found amount (mg)	20.05	5.03
Average recovery (%)	100.25	100.60
RSD% of recovery[a]	0.46	0.66
Bias%	0.25	0.60

[a]Each value is the mean of three experiments

the mixture of ESOM and using interference agents such as dopamine (DOP), ascorbic acid (AA), Na$^+$, SO$_4^{2-}$, paracetamol (PAR), and uric acid (UA). *I* = *Im/Io* and RSD (%) values were calculated by mixing the ingredients showing interference influence ESOM at a rate of 1:10. As given in Table 4, relative error values were acquired between 98.72 and 100.48%. These results demonstrated that interfering substances with ten times of the ESOM concentration would not interfere with ESOM detection, revealing the good anti-interference ability of the SiO$_2$-β-CD@MIP/GCE sensor. The proposed SiO$_2$-β-CD@MIP/GCE sensor was applied nearly identically to the peak signal in the lack of interference agents.

Stability

Precision studies were carried out to determine the reproducibility of the developed method. Repeatability was evaluated by testing an SiO$_2$-β-CD@MIP/GCE sensor for five replicated determinations. The RSD value for the 1×10^{-14} M ESOM five measurements is 0.328%. Reproducibility was evaluated by determining the response of five different
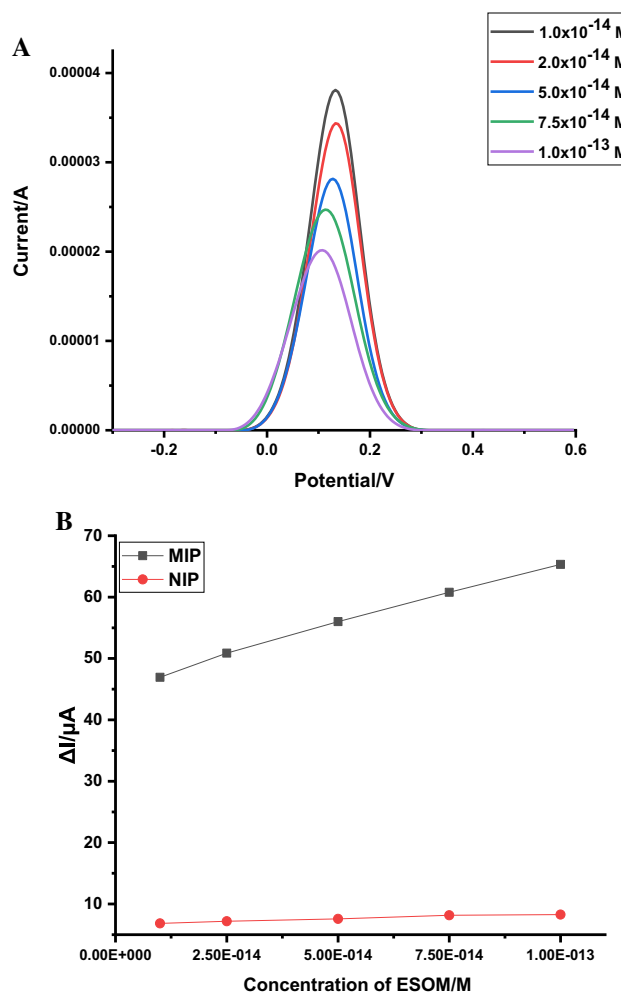
Fig. 7 DPV of ESOM on the SiO$_2$-β-CD@MIP/GCE (**A**) and a linear relationship between the ΔI and ESOM concentrations at SiO$_2$-β-CD@MIP/GCE and NIP/GCE (**B**) in spiked serum samples

electrodes immersed in 1×10^{-14} M ESOM. The RSD for five consecutive experiments is 0.524%, respectively, indicating acceptable repeatability of electrode fabrication.

Table 3 Recent electrochemical studies about esomeprazole

Sensor	Method	Linear range	LOD	Ref
rGO/CHNF/CPE	SWAdSV	$1.5–105\times10^{-8}$ M	5×10^{-9} M	[11]
PANI-ZrO$_2$/GCE	CV	200 ng mL^{-1} to 1.2 µg mL^{-1}	97.21 ng mL^{-1}	[12]
AuE	SWV	3.0 to 500 µg mL^{-1}	1.4 µg mL^{-1}	[13]
SPCE	DPV	$1.0\times10^{-6}–1.0\times10^{-4}$ M	3.5×10^{-8} M	[14]
P-β-CD-L-arg/SPCE	DPAdSV	$1.0\times10^{-8}–1.0\times10^{-5}$ M	3.0×10^{-9} M	[15]
SiO$_2$-β-CD@MIP/GCE	DPV	$1\times10^{-14}–2\times10^{-13}$ M	1.89×10^{-15} M	This work

AuE gold electrode, *CHNF* Co(OH)$_2$ nano-flakes, *DPAdSV* differential pulse adsorptive stripping voltammetry, *PANI* polyaniline, *rGO* reduced graphene oxide, *SPCE* screen-printed carbon electrode, *SWV* square wave voltammetry, *SWAdSV* square wave adsorptive stripping voltammetry, *ZrO$_2$* zirconia

Table 4 Effect of interfering agents on the detection of ESOM

Interference agents	$I = Im/Io$	RSD (%)
DOP	99.86	0.54
AA	98.72	0.47
Na$^+$	99.35	0.38
SO$_4^{2-}$	98.76	0.40
PAR	100.24	0.57
UA	100.48	0.68

The stability of the developed sensor is critical for its practical application. The stability of the electrode was investigated by measuring the current response of the sensor at day 1, 3, 5, 7, and 10 after fabrication. Between measurements, the electrode was stored at room temperature at 25 °C. The current response decreased to 95.39% after 5 days, while 86.56% of the original response was maintained after 10 days.

Conclusion

A novel SiO$_2$-β-CD@MIP/GCE sensor was developed for ultrasensitive and selective detection of ESOM using a simple and cost-effective molecular imprinting approach. In selectivity study, imprinting factor of SiO$_2$-β-CD@MIP/GCE toward ESOM with respect to R-OM, S-lansoprazole, and R-lansoprazole was determined as 5.81, 1.33, 1.03, and 1.26, respectively. The storage stability of the sensor has remained as 86.56% after 10 days, indicating it could be repeatedly used with no significant decrease in their performance. Hence, the developed MIP sensor showed great analytical performance with significant selectivity, anti-interference ability, stability, and reproducibility, holding great promise for applications in the pharmaceutical industry. Moreover, the first attempt of applying the MIP approach in the field of chiral electrochemical sensors to detect ESOM may provide new insight into the design and application of the MIP sensor for the detection of ESOM. The practical application of the sensor also showed good reproducibility and stability for the detection of ESOM in serum and tablet samples. These results showed proposed sensor was successfully applied for the selective recognition of ESOM in biological and pharmaceutical samples with high sensitivity and excellent selectivity. As a result, very low LOD and LOQ values were obtained in both standard solution and serum samples compared to other studies available in the literature. Furthermore, imprinting factor and interference studies confirmed the selectivity of the sensor. Consequently, this newly developed sensor is a novel, sensitive, selective, and stable option for the analysis of ESOM even at very low concentrations. The limitation of the developed sensor is that the concentration range is narrow. The main challenge remains to create MIPs in large batches that are homogenous in size and shape but also in their affinity towards their target.

Declarations

Conflict of interest The authors declare no competing interests.

References

1. Nguyen LA, He H, Pham-Huy C (2006) Chiral drugs: an overview. Int J Biomed Sci 2:85
2. Asghar W, Pittman E, Jamali F (2015) Comparative efficacy of esomeprazole and omeprazole: racemate to single enantiomer switch. DARU J Pharm Sci 23:. https://doi.org/10.1186/S40199-015-0133-6
3. Mizunashi K, Furukawa Y, Katano K, Abe K (1993) Effect of omeprazole, an inhibitor of H+, K(+)-ATPase, on bone resorption in humans. Calcif Tissue Int 53:21–25. https://doi.org/10.1007/BF01352010

4. Manoli K, Magliulo M, Torsi L (2013) Chiral sensor devices for differentiation of enantiomers. Top Curr Chem 341:133–176. https://doi.org/10.1007/128_2013_444

5. Kaya SI, Corman ME, Uzun L, Ozkan SA (2022) A porous molecularly imprinted electrochemical sensor for specific determination of bisphenol S from human serum and bottled water samples in femtomolar level. Anal Bioanal Chem 414:2775–2785. https://doi.org/10.1007/S00216-022-03928-5/TABLES/5

6. Armutcu C, Özgür E, Çorman ME, Uzun L (2021) Interface imprinted polymers with well-oriented recognition sites for selective purification of hemoglobin. Colloids Surf B Biointerfaces 197:111435. https://doi.org/10.1016/J.COLSURFB.2020.111435

7. Ermiş N, Uzun L, Denizli A (2017) Preparation of molecularly imprinted electrochemical sensor for l-phenylalanine detection and its application. J Electroanal Chem 807:244–252. https://doi.org/10.1016/J.JELECHEM.2017.11.025

8. Lowdon JW, Diliën H, Singla P et al (2020) MIPs for commercial application in low-cost sensors and assays — an overview of the current status quo. Sensors Actuators B Chem 325:128973. https://doi.org/10.1016/J.SNB.2020.128973

9. Hamad M, Al-Sharqawi A, Dayyih WA et al (2016) Simultaneous estimation of esomeprazole and tadalafil in pharmaceutical formulations using high performance liquid chromatography. J Appl Pharm Sci 6:52–59. https://doi.org/10.7324/JAPS.2016.60407

10. Jain DK, Jain N, Charde R, Jain N (2011) The RP-HPLC method for simultaneous estimation of esomeprazole and naproxen in binary combination. Pharm Methods 2:167–172. https://doi.org/10.4103/2229-4708.90356

11. Mabrouk MM, Hammad SF, Mansour FR, El-Khateeb BZ (2019) Simultaneous determination of diclofenac and esomeprazole by reversed phase liquid chromatography, Dual Wavelength and Derivative Spectrophotometry. J Anal Chem 74:458–466. https://doi.org/10.1134/S1061934819050071

12. Nisar N, Sohail K, Bashir S, Shah SNH (2019) Simultaneous monitoring of esomeprazole and ondansetron in rabbit plasma by high performance liquid chromatography (HPLC) method. Lat Am J Pharm 38:342–349

13. Raman NVVSS, Reddy KR, Prasad AVSS, Ramakrishna K (2008) Development and validation of a GC-MS method for the determination of methyl and ethyl camphorsulfonates in esomeprazole magnesium. Chromatographia 68:675–678. https://doi.org/10.1365/s10337-008-0756-6

14. El-Wekil MM, Alkahtani SA, Ali HRH, Mahmoud AM (2018) Advanced sensing nanomaterials based carbon paste electrode for simultaneous electrochemical measurement of esomeprazole and diclofenac sodium in human serum and urine samples. J Mol Liq 262:495–503. https://doi.org/10.1016/j.molliq.2018.04.120

15. Jain R, Tiwari DC, Shrivastava S (2014) A sensitive voltammetric sensor based on synergistic effect of polyaniline and zirconia nanocomposite film for quantification of proton pump inhibitor

16. Ivić MA, Lović J, Stevanović S, et al (2019) Electrochemical behavior of esomeprazole: its determination at Au electrode as standard and in injection powder combined with the study of its degradation. undefined 848:. https://doi.org/10.1016/J.JELECHEM.2019.113303

17. Radi A, Abd-Elkader A (2015) Voltammetric behaviour of esomeprazole at screen printed carbon electrode and its determination in capsule dosage form. Eurasian J Anal Chem 9(2):92–101

18. Radi AE, El-Ghany NA, Wahdan T (2016) Determination of Esomeprazole on an electropolymerized L-arginine and β-cyclodextrin modified screen printed carbon electrode. Electroanalysis 28:1112–1118. https://doi.org/10.1002/ELAN.201501074

19. Dudhe PB, Shinde AP, Salgar K (2014) Development and validation of analytical methods for simultaneous estimation of domperidone and esomeprazole magnesium in bulk and in pharmaceutical formulations using UV-visible spectroscopy. Int J PharmTech Res 6:1501–1508

20. Jain N, Kulkarni S, Jain DK, Jain SK (2012) Spectrophotometric methods for simultaneous estimation of esomeprazole magnesium and naproxen in a tablet dosage form. Acta Pol Pharm Drug Res 69:1195–1199

21. Zhao X, Wang Y, Zhang P et al (2021) Recent advances of molecularly imprinted polymers based on cyclodextrin. Macromol Rapid Commun 42:2100004. https://doi.org/10.1002/MARC.202100004

22. Feng XP, Guo YF, Qian R et al (2021) Immobilized β-cyclodextrin and palladium-pyridylaldehyde complex on silica nanoparticles as a highly active catalyst for Suzuki, reduction of nitroarenes and oxidative amination of aldehydes reactions in water. Mater Today Commun 26:101909. https://doi.org/10.1016/j.mtcomm.2020.101909

23. Jiang Y, Liang Y, Zhang H et al (2014) Preparation and biocompatibility of grafted functional β-cyclodextrin copolymers from the surface of PET films. Mater Sci Eng C 41:1–7. https://doi.org/10.1016/j.msec.2014.04.031

24. Ozkan SA, Kauffmann J-M, Zuman P (2015) Electroanalytical method validation method validation in pharmaceutical analysis and their applications. Springer, Berlin, pp 235–266

25. (1995) ICH Topic Q 2 (R1) Validation of analytical procedures: text and methodology Step 5 note for guidance on validation of analytical procedures: text and methodology (CPMP/ICH/381/95) approval by CPMP November 1994 DATE for coming into operation